Image guided surgery: clinical validation of lesion identification technologies and exploration of nerve sparing approaches

KleinJan, G.H.

Author: KleinJan, G.H.
Title: Image guided surgery: clinical validation of lesion identification technologies and exploration of nerve sparing approaches
Issue Date: 2018-03-08

Chapter 9

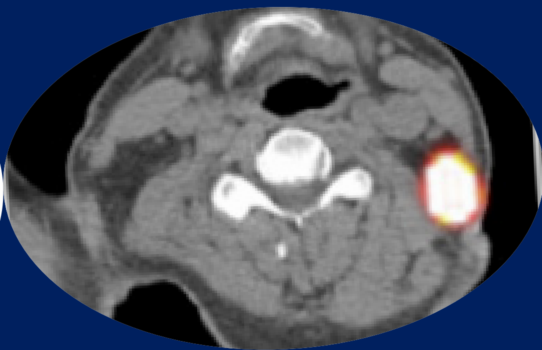

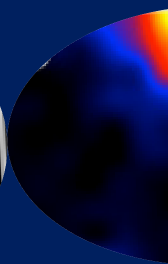

Extending the use of hand-held gamma camera technologies to generate intraoperative freehandSPECT images suitable for surgical navigation; a feasibility study in head-and-neck melanoma patients undergoing sentinel node biopsy

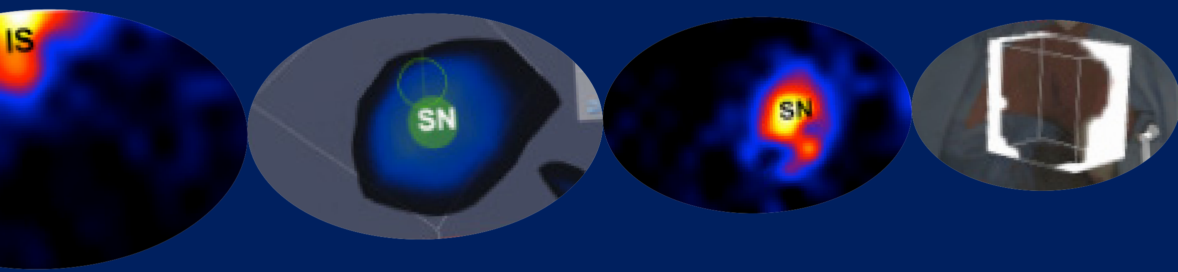

Gijs H. KleinJan
Baris Karakullukçu
W. Martin C. Klop
Thijs Engelen
Nynke S. van den Berg and
Fijs W.B. van Leeuwen
EJNMMI Res. 2017 17;7(1):65.

ABSTRACT

INTRODUCTION
Intraoperative sentinel node (SN) identification in patients with head-and-neck malignancies can be challenging due to unexpected drainage patterns and the anatomical complexity. Here, intraoperative navigation-based guidance technologies may provide outcome. In this study gamma-camera-based freehandSPECT was evaluated in combination with the hybrid tracer ICG-^{99m}Tc-nanocolloid.

MATERIALS AND METHODS
Eight patients with melanoma located in the head-and-neck area were included. Indocyanine green (ICG)-^{99m}Tc-nanocolloid was injected preoperatively, where after lymphoscintigraphy and SPECT/CT imaging were performed in order to define the location of the SN(s). FreehandSPECT scans were generated in the operation room using a portable gamma camera. For lesion localization during surgery freehandSPECT scans were projected in an augmented reality video-view that was used to spatially position a gamma-ray detection probe. Intraoperative fluorescence imaging was used to confirm the accuracy of the navigation-based approach and identify the exact location of the SNs.

RESULTS
Preoperatively fifteen SNs were identified, of which fourteen were identified using freehandSPECT. Navigation towards these nodes using the freehandSPECT approach was successful in thirteen nodes. Fluorescence imaging provided optical confirmation of the navigation accuracy in all patients. In addition, fluorescence imaging allowed for the identification of (clustered) SNs that could not be identified based on navigation alone.

CONCLUSION
The use of gamma camera-based freehandSPECT aids intraoperative lesion identification, and with that, supports the transition from pre- to intra-operative imaging via augmented reality display and directional guidance.

INTRODUCTION

Over the past decades the sentinel node (SN) biopsy procedure for loco-regional lymph node (LN) staging in patients with (head-and-neck) melanoma has increasingly gained interest [1,2]. This procedure allows preoperative identification of the primary tumor draining LNs (so-called sentinel nodes (SNs)) using lymphoscintigraphy and single photon emission computed tomography combined with computed tomography (SPECT/CT) imaging [3]. This information can then be used to provide the base for a surgical roadmap.

Differences in patient placement during preoperative imaging and head and neck surgery complicates the direct translation of the pre-operative findings to the surgical field of view. Intraoperative guidance is therefore required in the form of a gamma-ray detection probe (referred to as gamma probe) [4,5] or portable/handheld gamma cameras that provide a superior sensitivity and high resolution [6,9]. Both techniques, however, lack in depth information; features that can be complemented through the use of superficial optical imaging/fluorescence guidance. Conversely, fluorescence imaging is limited by tissue induced signal attenuation, making the technology dependent on other in depth imaging technologies such as SPECT.

In order to provide placement of radioactive hot spots into anatomical context optical and gamma tracing modalities can be physically integrated [10–12]. Alternatively, navigation of surgical tools/modalities in a manner analogue to the use of global positioning systems (GPS) instead of an old-fashion paper road-map can be employed. Navigation was successfully introduced in radioguided surgery via the use of geometrically tracked gamma probe's that generate freehandSPECT scans that can be presented as augmented reality views [13–16]. Uniquely, these 3D data-sets also allow for surgical navigation by providing dynamic feedback with regard to the distance of the gamma probe to the lesion of interest e.g. SN's of head-and-neck malignancies [14,17,18]. Limiting factors in the practical application of this technology are the sensitivity and the time that is required to generate a freehandSPECT scan. Recently we presented that, in breast cancer, intraoperative use of a handheld gamma camera rather than a gamma probe for freehandSPECT acquisition could overcome these shortcomings [6]. Others have used this approach for SN biopsy in different malignancies and for the detection of parathyroid adenoma [19–21].

In the current clinical pilot study, the feasibility of the use of a handheld gamma camera for intraoperative freehandSPECT acquisition and subsequent navigation-guided surgery was explored in patients with head-and-neck melanoma. Indocyanine green (ICG)-^{99m}Tc-nanocolloid was used to help validate the accuracy of the navigation procedure, as this tracer can be detected using both freehandSPECT and high-resolution fluorescence imaging [22].

METHODS

Patients

Eight patients with histology-proven melanoma in the head-and-neck area whom were scheduled for wide re-excision of the melanoma scar and a SN biopsy procedure were included (for patient characteristics see Table 1). Clinically, the regional LNs of the patients were tumor-negative as defined by palpation, ultrasound and fine-needle aspiration cytology.

Prior to commencement of the study, approval from the institutional review board of The Netherlands Cancer Institute - Antoni van Leeuwenhoek was obtained and patients were only included after written informed consent was provided.

Preoperative procedure

Preparation and injection of the hybrid tracer ICG-^{99m}Tc-nanocolloid, as well as the applied preoperative imaging procedure have previously been described [22]. ICG-^{99m}Tc-nanocolloid was injected intradermally in four deposits (0.1 mL/deposit) surrounding the melanoma scar. Lymphoscintigraphy (15 min and 2 h post-injection) and SPECT/CT imaging (2 h post-injection) were performed in order to determine the number and location of the SN-related hot spots. For SPECT/CT acquisition, the patient was placed in a supine position, with a straight neck. Preoperative findings are provided in Table 1.

				Preoperative findings				Intraoperative findings					Pathology	
	Age	Clinical T-stage	Tumor location	Administered dose (MBq)	# SNs on lymphoscintigrams	# SNs on SPECT/CT	Location SNs	Total # removed SNs	Fluorescent SNs		Radioactive SNs		Total # SNs	# Tumor-positive nodes
									In vivo	Ex vivo	In vivo	Ex vivo		
1	60	T2a	Right cheek	82.0	0	4	Parotid gland (2x), level I (2x)	4	3	4	4	4	4	0
2	74	T2b	Left cheek	84.9	3	3	Parotid gland, level II, level V	4	4	4	4	4	6	0
3	67	-	Right eyelid	84.4	1	1	Parotid gland	1	1	1	1	1	1	0
4	52	T3b	Right cheek	78.2	1	1	Level V	1	1	1	1	1	1	0
5	59	T4b	Left occipital region	90.2	1	1	Level V	1	1	1	1	1	1	1
6	63	T3a	Right occipital region	101.4	0	1	Level II	3	3	3	3	3	4	0
7	66	T2a	Vertex	75.5	2	2	Level II (2x)	3	3	3	3	3	4	0
8	43	T3a	Left ear	90.1	2	2	Parotid gland, level II	3*	3	3	3	3	3	1
Average	60.5			85.8	1.25	1.9		2.5	2.4	2.5	2.5	2.5	3	
Total					10	15		20	19	20	20	20	24	2

Table 1. Patient characteristics, preoperative and intraoperative findings, and pathology

MBq = mega Bequerel; SN = sentinel node; SPECT/CT = single photon emission computed tomography combined with computed tomography.

* Additional SN near injection site found with transcutaneous fluorescence imaging (and confirmed using the gamma probe) which was not seen on preoperative imaging.

9

Intraoperative procedure

Reference tracker placement

Placement of reference trackers for acquiring freehandSPECT images and the set-up for navigation were carried out according to procedures described by Engelen et al. [6]. In short, after anesthetizing the patient and sterilizing the operation field, the neck of the patient was positioned in such a way that the surgeon had easy access to the SNs on one side of the neck. Thereafter a sterile reference tracker (referred to as RT_p) was placed on the skull of the patient, followed by placement of a second reference tracker (referred to as RT_{hgc}) onto the handheld gamma camera (ChrystalCam; Chrystal Photonics, Berlin, Germany). Finally, a third reference tracker (referred to as RT_{gp}) was placed on the gamma probe (Chrystal probe; Chrystal Photonics).

To ensure continuous capture of all reference trackers in the field of view the navigation system, the optical tracking system was placed in direct line of site with the RTp., above the head of the patient. Near-infrared optical tracking of the fiducials present on the RT_p, the RT_{hgc}, and the RT_{gp}, the navigation system (declipseSPECT; SurgicEye, Munich, Germany) was used to determine the position and orientation of the patient, the handheld gamma camera and the gamma probe, and to place these features in the same coordinate system [6,23]. The tip of the gamma probe (approx. 1 cm in diameter) was used for navigation, as this allowed easier identification of the SNs compared to the use of the bulkier hand-held gamma camera.

FreehandSPECT acquisition in the head-and-neck area using a handheld gamma camera

The 2D gamma-imaging mode of the handheld gamma camera was used to roughly localize the area harboring the SNs and to center the radioactive hotspot in the volume of interest (VOI; 12x12x12 cm) of the freehandSPECT. After defining the position of the VOI, the geometrically tracked handheld gamma camera was used to scan the VOI in different directions whereby the declipseSPECT device provided feedback on the radioactive counts collected. When >2500 counts were collected, the acquisition was stopped and the freehandSPECT image reconstructed. Subsequently, the "tracked" gamma probe was navigated by the surgeon until the intact skin was reached. The accuracy of this position was then evaluated by comparing the position of the "tracked" gamma probe with that of a second gamma probe that was placed based on acoustic guidance.

Sentinel node identification: Navigation, gamma probe- and fluorescence-guidance
After incision, the SN was pursued using the conventional approach of combined gamma tracing (Neoprobe; Johnson & Johnson Medical, Amersfoort, the Netherlands) and fluorescence imaging (PhotoDynamic Eye (PDE); Hamamatsu Photonics K.K., Hamamatsu, Japan) in a manner similar as described previously [22]. When the SN was visible, the "tracked" gamma probe was navigated towards the SN using the freehandSPECT scan acquired prior to placement of the incision. The distance from the tip of the "tracked" gamma probe to the SN for each procedure, as reported by the navigation device, is provided in Table 2.

A post-excision freehandSPECT was generated after removal of the SNs to evaluate possible residual radioactivity present in the VOI. A mobile gamma camera (Sentinella; Oncovision, Valencia, Spain) was used to confirm removal of the preoperatively identified SNs [24].
The techniques used in this study and the type of information they provide during the surgical procedure are described in Table 3. Since the study entailed the evaluation of a new technology this resulted in the duplication of gamma-probe and -camera systems.

Pathology
Excised SN specimens were formalin-fixed and the nodes present in the specimens counted before being bisected and paraffin-embedded. Tissue sections cut at 50-150 nm intervals were used for histopathological evaluation and evaluation of the presence of nodal metastasis [22].

	Acquisition time (s)	% VOI scanned	Reconstruction time (s)	# SNs on freehandSPECT/total # SNs preoperative imaging (%)	# SNs located with navigation/# SNs seen on freehandSPECT (%)	Error of navigation per SN (mm)	Note
1	85	66.3	31	3/4 (75)	3/3 (75)	7, 8, 4	SN in parotid gland not visible on freehandSPECT
2	100	78	n.n.	3/3 (100)	3/3 (100)	9, 9, 9	Level V cluster of 2
3	121	67.6	87	1/1 (100)	1/1 (100)	5	-
4	126	51.5	211	1/1(100)	1/1 (100)	2	-
5	94	71	31	1/1(100)	1/1 (100)	5	-
6	74	59	89	1/1 (100)	0/1 (0)	-	SN part of IS, navigation not possible; level II SN cluster of 3
7	132	82	135	2/2 (100)	2/2 (100)	0, 5	Level II cluster of 2
8	199	80.4	90	2/2 (100)	2/2 (100)	7, 5	-
Average	116.4	69.5	96.3			5.8	
Total				14/15 (93.3)	13/14 (92.9)		

Table 2. Intraoperative freehandSPECT findings

SN = sentinel node; SPECT/CT = single photon emission computed tomography; VOI; = volume of interest; 3D = three-dimensional; n.n.

= not noted; IS = injection site

* = this SN was not reported by the nuclear medicine physician, but was visible on freehandSPECT.

	2D information	3D information	Acoustic read-out	Numerical read-out	Visual read-out	Depth information	Anatomical detail
Neoprobe gamma probe#,*	-	-	+	+	-	-	-
Sentinella gamma camera#,*	+	-	+	+	+ (gamma image)	-	-
PDE fluorescence camera#,*	+	-	-	-	+ (fluorescence image)	+/-	+
(Chrystal) gamma camera combined with freehandSPECT (incl. navigation of Chrystal gamma probe and acoustic confirmation with the same probe)#	+	+	+	+	+ (gamma image)	+	-
Fluorescence camera combined with freehandSPECT	+	+	+	+	+ (gamma + fluorescence image)	+	+

Table 3. Information provided by different intraoperative imaging modalities

2D = two-dimensional; 3D = three-dimensional. # Technologies applied in this study.* Routine modality used for the procedures describe in the study.

RESULTS

Preoperative imaging procedure

With preoperative lymphoscintigraphy and SPECT/CT imaging a total of 15 SN-related hot spots were identified (Table 1). Interestingly, in one patient (patient 1) non-visualization occurred on early- and late lymphoscintigrams while with SPECT/CT four SN-related hot spots were identified (Table 1).

Direct translation of the preoperative SPECT/CT scans to the surgical setting was not always possible, due to the difference in patient positioning during the preoperative SPECT/CT scan and the intervention. Complexity of translation further increased when SN-related hot spots were identified in both sides of the neck, which required repositioning of the patient during surgery in order to expose both sides of the neck. These features complicated the surgeons ability to relate anatomical reference points in preoperative SPECT/CT to those in the intraoperative situation.

Pre-incision imaging procedure

On average, freehandSPECT acquisition took a mere 116.4 seconds (range 74-199 seconds), in which an average of 69.5% of the VOI was scanned (range 51.5-82.0%). FreehandSPECT reconstruction time was on average 96.3 seconds (range 31-211 seconds; Table 2). As the patient was immobilized on the operation table, the acquired freehandSPECT scans were limited by the degree of freedom wherein the camera could be positioned over the lesion in order to generate a 3D image. Furthermore, the limited volume of interest of scanned (12x12x12 cm) resulted in the acquisition of multiple freehandSPECT in the first two patients.

Using preoperative SPECT/CT as a reference for identified SNs, intraoperatively obtained freehandSPECT images provided a 93% detection rate (14/15 SN-related hot spots visualized). When identified, the exact location of the SNs in the surgical set-up could be depicted as an augmented reality overlay. As demonstrated by a typical example in Figure 1, handheld gamma camera and freehandSPECT scans depicted the same features as the preoperatively acquired lymphoscintigrams and SPECT/CT images in 75% of patients (no complete conformity in patient 1 and 6).

In patient 1, four SN-related hot spots were preoperatively identified with SPECT/CT. In this patient, low tracer uptake in a SN located in the parotid gland prevented detection using freehandSPECT. In patient 6, a lower-activity SN-related hot spot near the high-activity injection site was identified on preoperative SPECT/CT which could also not be identified using freehandSPECT. A cluster of SN-related hot spots in level II was identified on preoperative SPECT/CT in patient 7, which could be differentiated into three SN-related hot spots after examination of the freehandSPECT scan.

Post-incision imaging procedure

Placement of the tracker on the rigid skull and outside the surgical field prevented the need for replacement during the surgical procedure and resulted in minimal deformations. The "tracked" gamma probe could be virtually navigated in seven patients (13 of the 14 SN-related hot spots (93%)) with a navigation inaccuracy of 5.8 mm in the numeric distance to the target (Table 2, Figures 1 and 2). It should be noted that this inaccuracy seemed to be influenced for a large part by the mere 3mm spatial resolution of the freehandSPECT images [25]. Inaccuracy induced by movement artifacts could be contributed to e.g. the incision process or retractors used. In all cases wherein the navigation procedure was slightly inaccurate identification of the SNs was enabled by a manual correction based on fluorescence imaging.

In cases wherein the navigation option could not be used, the combined use of the SPECT/CT images, gamma probe and fluorescence camera allowed identification of the SNs (Table 2). In patients 1 and 6, the superior spatial resolution of fluorescence imaging allowed localization of the SNs that were not detected by freehandSPECT. In patient 6, intraoperative fluorescence imaging revealed three SNs at the location of the hotspot that was identified on SPECT/CT. Post-SN-excision freehandSPECT and use of the alternative mobile gamma camera, confirmed accurate removal of the SNs in all patients.

Pathology

Pathological evaluation of the biopsy specimens resulted in identification of a total of 24 nodes, of which two were tumor-positive (found in patient 5 and 8; Table 1). In patient 8, a tumor-positive SN was found in the parotid gland, while in patient 5 a tumor-positive node was located in the re-excision specimen of the melanoma scar. This last node was overshadowed by the high-activity of the injection site, which prevented identification on preoperative images and was therefore not explored during the operation.

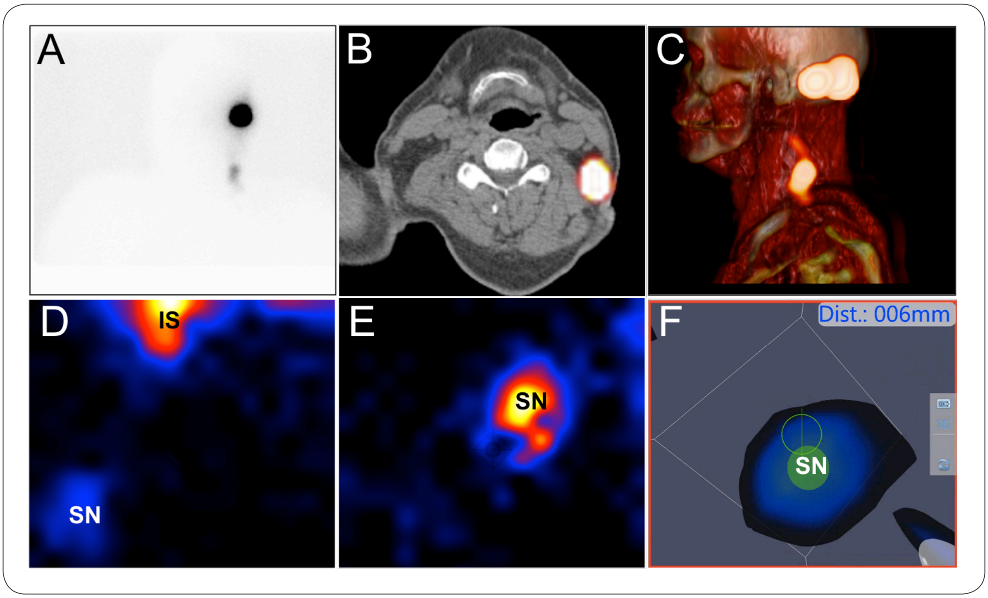

Figure 1. Overview of the acquired images.

A. Example of an anterior lymphoscintigram showing a clear sentinel node in the neck.

B, C. SPECT/CT imaging of the patient shown under A allowed to place the hotspot in its anatomical context with the sentinel node being located in level V. The fused SPECT/CT images provided the surgeon with an anatomical roadmap for planning of the surgical procedure.

D. 2D mobile gamma camera image acquired in the operation room showing a sentinel node (SN) and the injection site (IS).

E. Zoom-in of the image shown in D.

F. A freehandSPECT scan was acquired and subsequently the gamma probe was navigated, in augmented reality, to the sentinel node as seen in the freehandSPECT scan.

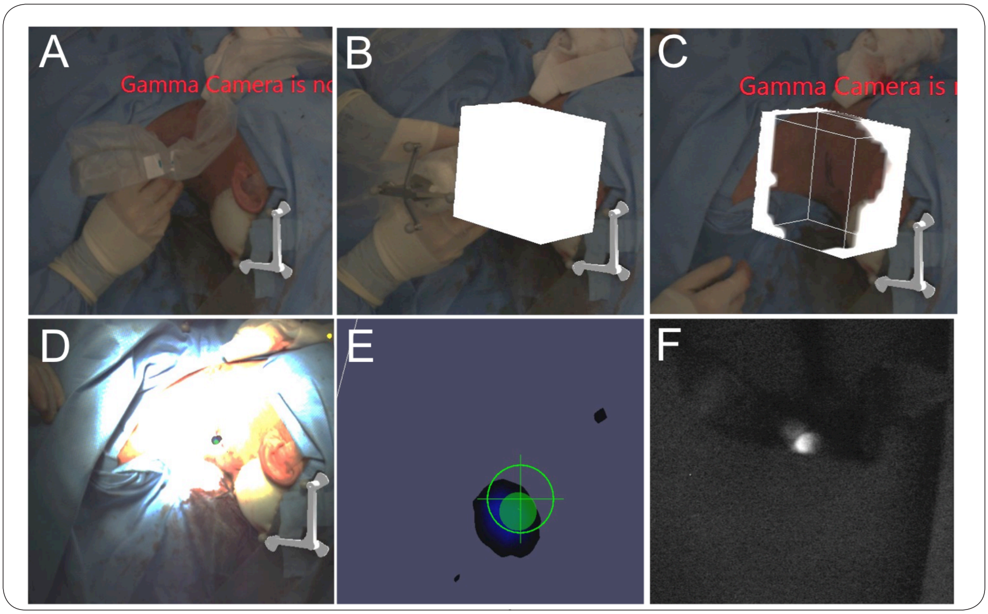

Figure 2. Intraoperative navigation procedure.

A. Pre-navigation overview.

B, C Intraoperative freehandSPECT acquisition.

D. Augmented reality following reconstruction of the acquired data, a 3D overlay is obtained.

E. Navigation of the gamma probe in 3D-virtual-reality.

F. Optical confirmation of sentinel node localization via fluorescence imaging.

DISCUSSION

The results described in this study demonstrate that intraoperative freehandSPECT scans that are generated using a handheld gamma camera provide a 93% detection-rate of SNs that were preoperatively identified on SPECT/CT identified in the head-and-neck area. The use of the hybrid tracer ICG-^{99m}Tc-nanocolloid allowed for the (high-resolution) detection of the remaining SNs using fluorescence imaging. During the surgical procedure, the freehandSPECT device helped to place the nuclear medicine findings within the anatomical context. In addition, the use of an augmented reality overlay lso provided dynamic information with regard to the distance to the target.

Due to the common occurrence of so-called clustered nodes in the head and neck area [22], there continues to be a discrepancy between the SN-related hot spots identified at SPECT/CT and the actual number of SN's removed during surgery (38% increase in this particular study; 24 in Table 1 vs. 15 in Table 2)). Unfortunately, intraoperative use of freehandSPECT did not demonstrate the resolution and real-time confirmation that is required to solve this issue. Hence, resection of all SNs in one hot spot still demands the use of high-resolution and real-time feedback, as is provided by fluorescence imaging.

When using preoperative SPECT/CT scans for navigation purposes identical RTp placement in the pre- and intra-operative setting was required to limit the degree of deformations [26–29]. This practical limitation was now overcome by the use of intraoperatively generated freehandSPECT scans. Unfortunately, the relatively small volume of interest of the freehandSPECT (12x12x12 cm) resulted in the generation of multiple freehandSPECT scans in some patients. The disruption of the surgical workflow was minimized by the prior knowledge of the location wherein the SNs resided. Such disruption, however, remains common during the introduction of new technologies and can be contributed to the early stage development of the technology as well as the limited experience with the technology (learning curve). It may be envisioned that integration of the freehandSPECT and navigation options in the surgical workflow can be optimized further form a technical point of view. For example, prevention of duplication of modalities (See Table 3) would already save time. Based on the fact that surgeons used the depth estimation provided by the navigation set-up to estimate the risk of damage to delicate tissues, one may also reason that striking a balance between cure and surgery induced toxicity would warrant a slight prolongation of the surgical procedure.

Previously we demonstrated that preoperative SPECT/CT remains incremental in the SN identification process, even when fluorescence-based surgical guidance to the same target is available [22]. Given the revealed need for positional information during placement of the freehandSPECT VOI we see no reason to deviate from this view. This study, however, does illustrate how freehandSPECT imaging and the matching "GPS-like" navigation capabilities can help strengthen the connection between the findings of both modalities [30]. The use of the hybrid tracer (ICG-^{99m}Tc-nanocolloid), a tracer that can be detected using both modalities [26], enabled complementary use of nuclear and fluorescent technologies. In the current study a gamma probe was used for navigation, but in the future other tools may be positioned using navigation, for example a fluorescence camera that displays a real-time augmented reality overlay of freehandSPECT data within the fluorescence images (see Table 3) [28]. In such an integrated image guided surgery approach the use of augmented reality displays, virtual navigation and fluorescence guidance can all be used in the same setting [31].

CONCLUSION

Generation of an intraoperative freehandSPECT scan using the handheld gamma camera/navigation system allows for the identification of SNs in the head and neck area, with an accuracy that approaches that of conventional SPECT/CT. The augmented reality display and directional positioning options provided by the navigation system help refine lesion localization, compared to traditional radioguided surgery tools.

REFERENCES

1. de Bree E, de Bree R. Implications of the MSLT-1 for sentinel lymph node biopsy in cutaneous head and neck melanoma. Oral Oncol. 2015;51(7):629-33.
2. de Rosa N, Lyman GH, Silbermins D, Valsecchi ME, Pruitt SK, Tyler DM, et al. Sentinel node biopsy for head and neck melanoma: a systematic review. Otolaryngol Head Neck Surg. 2011;145(3):375-82
3. Nieweg OE, Tanis PJ, Kroon BB. The definition of a sentinel node. Ann Surg Oncol. 2001;8(6):538-41.
4. Povoski SP, Neff RL, Mojzisik CM, O'Malley DM, Hinkle GH, Hall NC, et al. A comprehensive overview of radioguided surgery using gamma detection probe technology. World J Surg Oncol. 2009;27;7:11
5. Tsuchimochi M, Hayama K. Intraoperative gamma cameras for radioguided surgery: technical characteristics, performance parameters, and clinical applications. Phys Med. 2013;29(2):126-38.
6. Engelen T, Winkel BM, Rietbergen DD, KleinJan GH, Vidal-Sicart S, Olmos RAV, et al. The next evolution in radioguided surgery: breast cancer related sentinel node localization using a freehandSPECT-mobile gamma camera combination. Am J Nucl Med Mol Imaging. 2015;15;5(3):233-45.
7. Heller S, Zanzonico P. Nuclear probes and intraoperative gamma cameras. Semin Nucl Med. 2011;41(3):166–81.
8. Tsuchimochi M, Hayama K. Intraoperative gamma cameras for radioguided surgery: technical characteristics, performance parameters, and clinical applications. Phys Med. 2013;29(2):126-38.
9. Hellingman D, de Wit-van der Veen LJ, Klop WMC, Olmos RAV. Detecting near-the-injection-site sentinel nodes in head and neck melanomas with a high-resolution portable gamma camera. Clin Nucl Med. 2015;40(1):e11-6.
10. Hellingman D, Vidal-Sicart S, de Wit-van der Veen LJ, Paredes P, Valdés Olmos RA. A New Portable Hybrid Camera for Fused Optical and Scintigraphic Imaging: First Clinical Experiences. Clin Nucl Med. 2016;41(1):e39-43.
11. KleinJan GH, Hellingman D, van den Berg NS, van Oosterom MN, Hendricksen K, Horenblas S, et al. Hybrid Surgical Guidance: Does Hardware Integration of γ- and Fluorescence Imaging Modalities Make Sense? J Nucl Med. 2017;58(4):646–50.
12. Lees JE, Bassford DJ, Blake OE, Blackshaw PE, Perkins AC. A Hybrid Camera for simultaneous imaging of gamma and optical photons. J Instrum. 2012;7(6):P06009–P06009.
13. Bluemel C, Herrmann K, Kübler A, Buck AK, Geissinger E, Wild V, et al. Intraoperative 3-D imaging improves sentinel lymph node biopsy in oral cancer. Eur J Nucl Med Mol Imaging. 2014;41(12):2257–64.
14. Bluemel C, Herrmann K, Müller-Richter U, Lapa C, Higuchi T, Wild V, et al. Freehand SPECT-guided sentinel lymph node biopsy in early oral squamous cell carcinoma. Head Neck. 2014;36(11):E112-6.
15. Bluemel C, Schnelzer A, Okur A, Ehlerding A, Paepke S, Scheidhauer K, et al. Freehand SPECT for image-guided sentinel lymph node biopsy in breast cancer. Eur J Nucl Med Mol Imaging. 2013;40(11):1656–61.
16. Okur A, Ahmadi S-A, Bigdelou A, Wendler T, Navab N. MR in OR: First analysis of AR/VR visualization in 100 intra-operative Freehand SPECT acquisitions. 2011 10th IEEE Int Symp Mix Augment Real. IEEE; 2011 Oct;211–8.
17. de Bree R, Pouw B, Heuveling DA, Castelijns JA. Fusion of Freehand SPECT and Ultrasound to Perform Ultrasound-Guided Fine-Needle Aspiration Cytology of Sentinel Nodes in Head and Neck Cancer. AJNR Am J Neuroradiol. 2015;36(11):2153-8.
18. Heuveling DA, van Weert S, Karagozoglu KH, de Bree R. Evaluation of the use of freehand SPECT for sentinel node biopsy in early stage oral carcinoma. Oral Oncol. 2015;51(3):287–90.
19. Heuveling DA, Karagozoglu KH, van Schie A, van Weert S, van Lingen A, de Bree R. Sentinel node biopsy using 3D lymphatic mapping by freehand SPECT in early stage oral cancer: a new technique. Clin Otolaryngol. 2012;37(1):89–90.
20. Wendler T, Herrmann K, Schnelzer A, Lasser T, Traub J, Kutter O, et al. First demonstration of 3-D lymphatic mapping in breast cancer using freehand SPECT. Eur J Nucl Med Mol Imaging. 2010;37(8):1452–61.
21. Bluemel C, Kirchner P, Kajdi GW, Werner RA, Herrmann K. Localization of Parathyroid Adenoma With Real-Time Ultrasound: Freehand SPECT Fusion. Clin Nucl Med. 2016;41(3):e141-2.
22. van den Berg NS, Brouwer OR, Schaafsma BE, Mathéron HM, Klop WMC, Balm AJM, et al. Multimodal Surgical Guidance during Sentinel Node Biopsy for Melanoma: Combined Gamma Tracing and Fluorescence Imaging of the Sentinel Node through Use of the Hybrid Tracer Indocyanine Green-(99m)Tc-Nanocolloid. Radiology. 2015;275(2):521-9.

23. Waelkens P, van Oosterom MN, van den Berg NS, Navab N, van Leeuwen FW. Surgical Navigation: An Overview of the State-of-the-Art Clinical Applications. In: Herrmann K, Nieweg OE, Povoski SP, editors. Radioguided surgery. Springer International Publishing; 2016
24. Vermeeren L, Valdés Olmos RA, Klop WMC, Balm AJM, van den Brekel MWM. A portable gamma-camera for intraoperative detection of sentinel nodes in the head and neck region. J Nucl Med. 2010;51(5):700–3.
25. Bluemel C, Matthies P, Herrmann K, Povoski SP. 3D scintigraphic imaging and navigation in radioguided surgery: freehand SPECT technology and its clinical applications. Expert Rev Med Devices. 2016;13(4):339–51.
26. Brouwer OR, Buckle T, Bunschoten A, Kuil J, Vahrmeijer AL, Wendler T, et al. Image navigation as a means to expand the boundaries of fluorescence-guided surgery. Phys Med Biol. 2012;57(10):3123–36.
27. Brouwer OR, van den Berg NS, Mathéron HM, Wendler T, van der Poel HG, Horenblas S, et al. Feasibility of intraoperative navigation to the sentinel node in the groin using preoperatively acquired single photon emission computerized tomography data: transferring functional imaging to the operating room. J Urol. 2014;192(6):1810–6.
28. KleinJan GH, van den Berg NS, van Oosterom MN, Wendler T, Miwa M, Bex A, et al. Towards (hybrid) navigation of a fluorescence camera in an open surgery setting. J Nucl Med. 2016;57(10):1650-1653.
29. van den Berg NS, Engelen T, Brouwer OR, Mathéron HM, Valdés-Olmos RA, Nieweg OE, et al. A pilot study of SPECT/CT-based mixed-reality navigation towards the sentinel node in patients with melanoma or Merkel cell carcinoma of a lower extremity. Nucl Med Commun. 2016;37(8):812-7.
30. van den Berg NS, Valdés-Olmos R a, van der Poel HG, van Leeuwen FWB. Sentinel lymph node biopsy for prostate cancer: a hybrid approach. J Nucl Med. 2013;54(4):493–6.
31. van den Berg NS, Miwa M, Kleinjan GH, Sato T, Maeda Y, van Akkooij AC, et al. (Near-infrared) fluorescence guided surgery under ambient light conditions, a next step to embedment of the technology in clinical routine. Ann Surg Oncol. 2016 Aug;23(8):2586-95.

Part three

Nerve sparing surgery

10

11

12